Enhancing Indoor and Outdoor THz Communications with Beyond Diagonal-IRS: Optimization and Performance Analysis

Asad Mahmood, Thang X. Vu, Symeon Chatzinotas, Björn Ottersten
Interdisciplinary Centre for Security, Reliability and Trust (SnT), University of Luxembourg
{asad.mahmood, thang.vu, symeon.chatzinotas, bjorn.ottersten}@uni.lu

Abstract—This work investigates the application of Beyond Diagonal Intelligent Reflective Surface (BD-IRS) to enhance THz downlink communication systems, operating in a hybrid: reflective and transmissive mode, to simultaneously provide services to indoor and outdoor users. We propose an optimization framework that jointly optimizes the beamforming vectors and phase shifts in the hybrid reflective/transmissive mode, aiming to maximize the system sum rate. To tackle the challenges in solving the joint design problem, we employ the conjugate gradient method and propose an iterative algorithm that successively optimizes the hybrid beamforming vectors and the phase shifts. Through comprehensive numerical simulations, our findings demonstrate a significant improvement in rate when compared to existing benchmark schemes, including time- and frequency-divided approaches, by approximately 30.5% and 69.9% respectively and even outperforms the STAR-IRS system by 76.99%. This underscores the significant influence of IRS elements on system performance relative to that of base station antennas, highlighting their pivotal role in advancing the communication system efficacy.

Index Terms—Terahertz Communications, Intelligent Reflective Surfaces, Hybrid Beamforming Optimization, Indoor-Outdoor Wireless Connectivity

I. INTRODUCTION

IN the realm of future wireless communications, including beyond 5G (B5G) and 6G technologies, there is a drive to establish higher performance benchmarks and introduce novel application scenarios for societal digitization [1], [2]. Terahertz (THz) communication has received considerable attention for its potential to deliver ultra-high data rates, thereby addressing the spectrum scarcity and capacity limitations faced by current communication systems [3]. Despite its promise, the adoption of THz technology faces significant challenges due to the inherent properties of THz, such as severe attenuation by molecular absorption and limited penetration through wall/obstacle, which are characteristic of high-frequency propagation [4]. To overcome these challenges, intelligent reflecting surfaces (IRS) emerge as practical solution capable of adjusting their amplitude and phase to redirect signal transmission, thereby enhancing signal strength and coverage [5], [6].

To fully exploit the advantages of IRS technology in THz communications, Hao et al. [7] focus on optimizing the weighted sum rate in THz multiple input multiple output (MIMO) systems through hybrid beamforming and IRS phase shifts. Zhao et al. [8] proposed the time delay-based IRS scheme to mitigate the impact of beam quint in THz communication. Zhu et al. [3] develop a robust beamforming strategy for IRS-assisted simultaneous wireless information and power

transfer (SWIPT) in secure THz systems, with an emphasis on minimizing power consumption and adhering to outage constraints. Yuan et al. [9] propose an approach for calculating the ergodic secrecy rate in THz-enabled IRS-assisted non-terrestrial network (NTN), considering atmospheric and phase challenges. Despite these advancements, all of these research efforts consider the traditional IRS architecture, which is capable of transmitting signals in one direction. Moreover, as per [10], [11], a considerable amount of mobile data traffic, estimated to be between 80% and 96%, is generated indoors due to the prevalent indoor lifestyle of users. This underscores the need for efficient outdoor-to-indoor communication solutions.

To address this challenge, Xing et al. [12] and Chen et al. [13] have propelled the development of efficient architecture focusing on significant advancements in channel modeling and measurement for indoor THz and sub-THz communications. Concurrently, Yildirim et al. [14] and Shaikh et al. [15] have made notable contributions to this domain, primarily concentrating on the deployment of multiple IRS units, which, however, may not align with the principles of resource efficiency. To overcome the limitations of traditional IRS, Beyond Diagonal Intelligent Reflective Surfaces (BD-IRS) are introduced by Li et al. [16], [17], Nerini et al. [18], and Soleymani et al. [19] as a novel advancement and demonstrate superiority over traditional IRS. Meanwhile, the unique demands of THz networks, particularly the issue of higher frequency attenuation within buildings, require thorough consideration and investigation, as done by Wang et al. [20] on simultaneous transmission and reflecting (STAR)-IRS for enabling THz communication across varied user groups. This joint effort underscores a strong motivation to advance communication technologies, highlighting BD-IRS as a promising solution for the future's communication system, like THz.

Hence, motivated by the preceding discussion, this study investigates the utilization of fully connected BD-IRS operating in a hybrid mode, incorporating both reflective and transmission functionalities. This configuration enables the enhanced simultaneous servicing of indoor and outdoor users by efficiently reflecting and transmitting signals, thereby optimizing resource utilization and improving overall network performance. Subsequently, the main contributions of this work are summarized as follows:

- We develop a joint optimization framework aimed at facilitating simultaneous service to both indoor and outdoor users. This is achieved by jointly optimizing the hybrid beamforming vectors at the THz base station (BS) and the phase shifts of the BD-IRS operating in the hybrid

mode.

- To address the optimization challenge, we decompose the joint problem into subproblems, focusing on hybrid beamforming and IRS phase-shift control. These are tackled iteratively using the Block Coordinate Descent (BCD) method, allowing for a systematic solution to the original complex optimization problem.
- Our results indicate that the proposed approach significantly outperforms existing benchmark schemes, with improvements in rate of approximately 30.50% and 69.9%, over the time- and frequency-division approaches and 76.99% over the STAR-IRS, thereby highlighting the critical impact of IRS elements on system performance compared to BS antennas.

The paper is structured as follows. Section II details the system model and problem formulation. Section III outlines the proposed solution. The numerical results are presented in Section IV, followed by the conclusions in Section V.

II. SYSTEM MODEL

This study explores the utilization of BD-IRS in fully connected architecture to enhance THz downlink communication systems to provide service to N single antenna indoor / outdoor users, denoted $\mathcal{N} = \{1, 2, \ldots, N\}$, as depicted in Fig. 1. The THz base station (BS) is equipped with M antennas and M_{RF} RF chains where $M_{RF} \leq M$. It is noteworthy that the number of users served is inherently limited by the number of RF chains. BD-IRS comprises K elements and denoted by $\mathcal{K} = \{1, 2, \ldots, K\}$. Users are divided into two distinct groups based on their physical location: reflective (outdoor) users, indexed by $\mathcal{N}_r \subseteq \mathcal{N}$, and transmissive (indoor) users, indexed by $\mathcal{N}_t \subseteq \mathcal{N}$. Under the assumption of the acquisition of perfect channel state information (CSI) achieved by channel estimation techniques [8], [21], this scenario posits an upper bound solution. Since the number of RF chains is less than the number of antennas, a hybrid beamforming design must be adopted that entails initial signal processing via a digital beamformer $\mathbf{V}^{\mathrm{BB}} \in \mathbb{C}^{M_{\mathrm{RF}} \times N}$, followed by an analog beamformer $\mathbf{V}^{\mathrm{RF}} \in \mathbb{C}^{M \times M_{\mathrm{RF}}}$. Furthermore, due to the blockage, the BS can only transmit data to the users via the BD-IRS, where it concurrently reflects and transmits the signal to the intended user. In this context, the BD-IRS scattering matrix can be denoted as $\mathbf{\Theta}_{i_n} \in \mathbb{C}^{K \times K}$, where $i_n = t$ if $n \in \mathcal{N}_t$ and $i_n = r$ if $n \in \mathcal{N}_r$ subject to the constraint $\mathbf{\Theta}_r^H \mathbf{\Theta}_r + \mathbf{\Theta}_t^H \mathbf{\Theta}_t = \mathbf{I}_K$, which ensures energy conservation in both reflection and transmission processes. The signal received from the n-th user is given as follows:

$$y_n = \boldsymbol{h}_n^H \mathbf{\Theta}_{i_n} \boldsymbol{G} \boldsymbol{w}_n x_n + \sum_{n' \neq n} \boldsymbol{h}_n^H \mathbf{\Theta}_{i_n} \boldsymbol{G} \boldsymbol{w}_{n'} x_{n'} + \eta_n. \quad (1)$$

In (1), the beamforming vector $\boldsymbol{w}_n = \mathbf{V}^{\mathrm{RF}} \mathbf{V}_n^{\mathrm{BB}} \in \mathbb{C}^{M \times 1}$ represents the composite beamforming effect for the n-th user. The channel vectors $\boldsymbol{h}_n \in \mathbb{C}^{K \times 1}$ and $\boldsymbol{G} \in \mathbb{C}^{K \times M}$ represent the channel from the IRS to the user and from the BS to the IRS, respectively. The transmitted signal for the n-th user, x_n, adheres to the condition $\mathbb{E}\{x_n x_n^*\} = 1$, and the additive white Gaussian noise at the user is denoted by η_n.
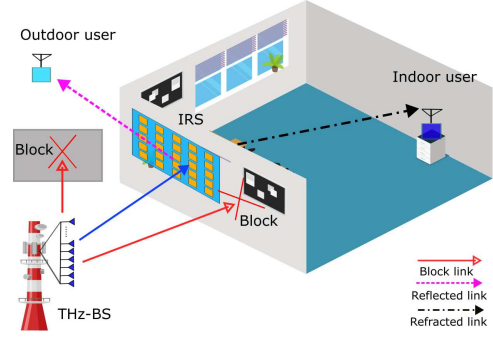

Fig. 1: System Model

Given the substantially lower power gain of non-line-of-sight (NLoS) paths compared to line-of-sight (LoS) paths in THz communications, this analysis primarily concentrates on the LoS channel model [3]. Hence, the channel $\boldsymbol{G}$ is modeled as $\boldsymbol{G} = q(f_c, d_1)\bar{\boldsymbol{G}}$, where $q(f_c, d_1) = \frac{c}{4\pi f_c d_1} e^{-\frac{1}{2}\tau(f_c)d_1}$ encapsulates the effects of free-space path loss and medium absorption. Here, c signifies the speed of light, f_c is the carrier frequency, d_1 represents the distance from the BS to the IRS, and $\tau(f_c)$ is the medium's absorption coefficient obtained from the high-resolution transmission (HITRAN) database [22]. The antenna array response vectors at the transmitter and IRS are represented by $\bar{\boldsymbol{G}} = \boldsymbol{a}_{\mathrm{tx}}(\vartheta_{\mathrm{tx}})\boldsymbol{a}_{\mathrm{rx}}^H(\vartheta_{\mathrm{rx}})$, defined for the respective angles of arrival and departure.

$$\boldsymbol{a}_{rx}(\vartheta_{rx}) = \left[1, e^{j\pi\vartheta_{rx}}, e^{j2\pi\vartheta_{rx}}, \ldots, e^{j(M-1)\pi\vartheta_{rx}}\right]^T, \quad (2)$$

$$\boldsymbol{a}_{tx}(\vartheta_{tx}) = \left[1, e^{j\pi\vartheta_{tx}}, e^{j2\pi\vartheta_{tx}}, \ldots, e^{j(K-1)\pi\vartheta_{tx}}\right]^T. \quad (3)$$

Here, $\vartheta_i = 2d_0 f_c \sin(\phi_i)/c, i \in \{rx, tx\}$, with d_0 representing antenna spacing, and $\phi_i \in [-\pi/2, \pi/2]$ denoting angle of departure (AoD) and angle of arrival (AoA), respectively. The channel vector $\boldsymbol{h}_n = q(f_c, d_2)\boldsymbol{a}_{\mathrm{tx}}(\vartheta_{\mathrm{tx}})$. Here d_2 denotes the distance between the IRS and users. Moreover, the signal-to-interference plus noise ratio (SINR) of n−th user can be expressed as:

$$\gamma_n = \frac{|\boldsymbol{h}_n^H \mathbf{\Theta}_{i_n} \boldsymbol{G} \boldsymbol{w}_n|^2}{\sum_{n' \neq n} |\boldsymbol{h}_n^H \mathbf{\Theta}_{i_n} \boldsymbol{G} \boldsymbol{w}_{n'}|^2 + \sigma^2}. \quad (4)$$

A. Problem Formulation

In this work, we aim to maximize the sum rate of the users by jointly optimizing the hybrid beamforming vector $\{\mathbf{V}^{\mathrm{RF}}, \mathbf{V}^{\mathrm{BB}}\}$, followed by an IRS scattering matrix $\mathbf{\Theta}_{t,r}$. Formulating the joint optimization problem as:

$$\max_{\mathbf{V}^{\mathrm{RF}}, \mathbf{V}^{\mathrm{BB}}, \mathbf{\Theta}_r, \mathbf{\Theta}_t} \sum_{n=1}^{N} \log_2\left(1 + \gamma_n\right) \quad (5a)$$

$$\text{s.t.} \, \mathbf{\Theta}_r^H \mathbf{\Theta}_r + \mathbf{\Theta}_t^H \mathbf{\Theta}_t = \boldsymbol{I}_K, \quad (5b)$$

$$\left\|\mathbf{V}^{\mathrm{RF}} \mathbf{V}^{\mathrm{BB}}\right\|_F^2 \leq P_{\max}, \quad (5c)$$

$$\left|\mathbf{V}^{\mathrm{RF}}(i, j)\right| = 1, \forall i, j, \quad (5d)$$

where γ_n is given in (4), $P_{\max}$ denotes the maximum allowable transmit power at the BS. The (5) poses substantial challenges because of nonconvex constraints along with the unitary nature of the IRS and the nonlinearity of the objective

function, as well as the coupling of variables detailed in (5c). To overcome these, we reformulate (5) into a more manageable form by using fractional programming techniques. Following this, an iterative method is employed to solve the reformulated problem efficiently. This approach facilitates a systematic enhancement of the sum rate for the users, achieved through the meticulous optimization of both the hybrid beamforming vector and the IRS scattering matrix.

III. PROPOSED SOLUTION

This section presents a proposed framework, in which we initially transform the objective function to more tractable by introducing auxiliary variables $\boldsymbol{\beta} \in \mathbb{R}^N = [\beta_1, \beta_2, \ldots, \beta_N]^T$ and $\boldsymbol{\alpha} \in \mathbb{C}^N = [\alpha_1, \alpha_2, \ldots, \alpha_N]^T$. Employing a quadratic transformation to convert the fractional SINR terms into an integer expression, we reformulate the (5a) as follows: [23, Sec. IV-C]

$$\mathcal{F}(\boldsymbol{\mathcal{X}}) = \sum_{n=1}^{N} (\log_2(1 + \beta_n) - \beta_n + \Gamma_n - \Xi_n), \qquad (6)$$

where $\boldsymbol{\mathcal{X}} = \{\mathbf{V}^{\text{RF}}, \mathbf{V}^{\text{BB}}, \boldsymbol{\Theta}_r, \boldsymbol{\Theta}_t, \boldsymbol{\beta}, \boldsymbol{\alpha}\}$ is the shorthand notation of the variables, $\Gamma_n = 2\sqrt{1+\beta_n}\,\text{Re}\left\{\alpha_n^\dagger \bar{\boldsymbol{h}}_n^H \boldsymbol{w}_n\right\}$, and $\Xi_n = |\alpha_n|^2 \sum_{n'\neq n} |\bar{\boldsymbol{h}}_n^H \boldsymbol{w}_{n'}|^2 + \sigma^2$; $\bar{\boldsymbol{h}}_n = (\boldsymbol{h}_n^H \boldsymbol{\Theta}_{i_n} \boldsymbol{G})^H$. Moreover, the new optimization problem expressed as:

$$\max_{\boldsymbol{\mathcal{X}}} \quad \mathcal{F}(\boldsymbol{\mathcal{X}}) \quad \text{s.t. Equations (5b) to (5d).} \qquad (7a)$$

Considering the multivariate complexity of (7), we adopt BCD to separate it into distinct subproblems. These subproblems are then iteratively addressed, with detailed explanations provided in the subsequent subsections.

A. Auxiliary Parameter Optimization

Under given $\mathbf{V}^{\text{RF}}, \mathbf{V}^{\text{BB}}, \boldsymbol{\Theta}_r$, and $\boldsymbol{\Theta}_t$, we optimize $\boldsymbol{\beta}$ and $\boldsymbol{\alpha}$ in the convex framework of (7). Setting the derivatives $\frac{\partial \mathcal{F}}{\partial \beta} = 0$ and $\frac{\partial \mathcal{F}}{\partial \alpha} = 0$ yields:

$$\beta_n^* = \gamma_n, \quad \alpha_n^* = \frac{\sqrt{1+\beta_n}\,\bar{\boldsymbol{h}}_n^H \boldsymbol{w}_n}{\sum_{n'\neq n} |\bar{\boldsymbol{h}}_n^H \boldsymbol{w}_{n'}|^2 + \sigma^2}. \qquad (8)$$

B. Hybrid Beamforming

In the realm of hybrid beamforming, the convexity of (6) facilitates the formulation of the optimization problem for $\mathbf{V}^{\text{RF}}$ and $\mathbf{V}^{\text{BB}}$ as follows:

$$\max_{\mathbf{V}^{\text{RF}}, \mathbf{V}^{\text{BB}}} \mathcal{F}(\mathbf{V}^{\text{RF}}, \mathbf{V}^{\text{BB}}) \quad \text{s.t. Equations (5c) and (5d).} \qquad (9a)$$

Despite the objective function's convexity, the coupling of decision variables presents a challenge to deriving optimal solutions. To mitigate this, subproblems are formulated, with a subset of variables being held constant as each subproblem is solved iteratively. Hence, the analog beamforming subproblem is specified as follows:

$$\max_{\mathbf{V}^{\text{RF}}} \quad \mathcal{F}(\mathbf{V}^{\text{RF}}) \quad \text{s.t. Equations (5c) and (5d).} \qquad (10a)$$
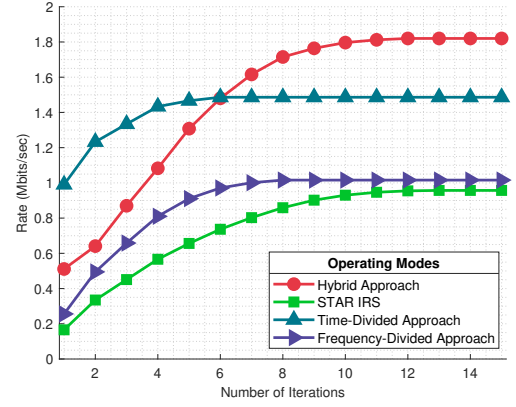

Fig. 2: Convergence Analysis

Similarly, the subproblem for digital beamforming is outlined as:

$$\max_{\mathbf{V}^{\text{BB}}} \quad \mathcal{F}(\mathbf{V}^{\text{BB}}) \quad \text{s.t. Equation (5c).} \qquad (11a)$$

Subproblems (10) and (11) are convex and can be solved iteratively using standard optimization tools, e.g., CVX.

C. IRS Phase Shift Optimization

Given $\mathbf{V}^{\text{RF}}, \mathbf{V}^{\text{BB}}, \boldsymbol{\beta}$, and $\boldsymbol{\alpha}$, we optimize $\boldsymbol{\Theta}_r$ and $\boldsymbol{\Theta}_t$ as follows:

$$\max_{\boldsymbol{\Theta}_r, \boldsymbol{\Theta}_t} \sum_{i_n} \left(2\,\text{Re}\{\text{Tr}(\boldsymbol{\Theta}_{i_n} \boldsymbol{X}_{i_n})\} - \text{Tr}(\boldsymbol{\Theta}_{i_n} \boldsymbol{Y} \boldsymbol{\Theta}_{i_n}^H \boldsymbol{Z}_{i_n})\right), \qquad (12a)$$

$$\text{s.t. Equation (5b),}$$

where $\boldsymbol{X}_{i_n} \in \mathbb{C}^{K \times K} = \sum_{n \in \mathcal{N}_{i_n}} \sqrt{1+\beta_n}\,\alpha_n \boldsymbol{G} \mathbf{V}^{\text{RF}} \mathbf{V}_n^{\text{BB}} \boldsymbol{h}_n^H$, $\boldsymbol{Y} \in \mathbb{C}^{K \times K} = \sum_{n'\neq n} \boldsymbol{G} \mathbf{V}^{\text{RF}} \mathbf{V}_{n'}^{\text{BB}} (\boldsymbol{G} \mathbf{V}^{\text{RF}} \mathbf{V}_{n'}^{\text{BB}})^H$, and $\boldsymbol{Z}_{i_n} \in \mathbb{C}^{K \times K} = \sum_{n \in \mathcal{N}_{i_n}} |\alpha_n|^2 \boldsymbol{h}_n \boldsymbol{h}_n^H$. Building on [17, Sec. IV-E], this simplify to $\boldsymbol{\Theta} = [\boldsymbol{\Theta}_t^H, \boldsymbol{\Theta}_r^H]^H$, $\boldsymbol{X} = [\boldsymbol{X}_t, \boldsymbol{X}_r]$, and $\boldsymbol{Z} = \text{blkdiag}(\boldsymbol{Z}_t, \boldsymbol{Z}_r)$, leading to the subproblem for $\boldsymbol{\Theta}$ as:

$$\max_{\boldsymbol{\Theta}} \mathcal{F}(\boldsymbol{\Theta}) = 2\,\text{Re}\{\text{Tr}(\boldsymbol{\Theta} \boldsymbol{X})\} - \text{Tr}(\boldsymbol{\Theta} \boldsymbol{Y} \boldsymbol{\Theta}^H \boldsymbol{Z}), \qquad (13a)$$

$$\text{s.t.} \quad \boldsymbol{\Theta}^H \boldsymbol{\Theta} = \boldsymbol{I}_K. \qquad (13b)$$

Utilizing the conjugate gradient ascent method [24], this strategy leverages the IRS elements to streamline the optimization of phase shifts. The initial step involves computing the Euclidean gradient of (13a), expressed as $\nabla \mathcal{F}(\boldsymbol{\Theta}) = 2\boldsymbol{X}^H - 2\boldsymbol{Z}\boldsymbol{\Theta}\boldsymbol{Y}$. This computation aids in determining the Riemannian gradient at $\boldsymbol{\Theta}$, formulated as: $\boldsymbol{J}(\boldsymbol{\Theta}) = \nabla \mathcal{F}(\boldsymbol{\Theta})\boldsymbol{\Theta}^H - \boldsymbol{\Theta}\nabla \mathcal{F}(\boldsymbol{\Theta})^H$. The Riemannian gradient, $\boldsymbol{J}(\boldsymbol{\Theta})$, then facilitates the calculation of the rotation matrix $\boldsymbol{R} = \boldsymbol{I} + \mu \boldsymbol{J} + \frac{\mu^2}{2}\boldsymbol{J}^2$, with μ serving as the control parameter for convergence. This rotation matrix is subsequently employed to iteratively update the IRS phase shift matrix as $\boldsymbol{\Theta}_l^{j+1} = \boldsymbol{J}(\boldsymbol{\Theta}^j)\boldsymbol{\Theta}^j$. Algorithm 1 outlines its operations and sets the worst case per iteration complexity at $\mathcal{O}(N^2 K^2 + I_1(M^{3.5} + (M_{\text{RF}}N)^3) + I_2 K^3)$, with I_1 and I_2 as the maximum iterations for hybrid beamforming and the conjugate gradient method, respectively. The function $\mathcal{F}(\boldsymbol{\mathcal{X}}^{t+1}) \geq \mathcal{F}(\boldsymbol{\mathcal{X}}^t)$ demonstrates that $\mathcal{F}$ iteratively converges towards a local optimum, with the pursuit of the global maximum identified as an area for further research.

Algorithm 1: Iterative Algorithm to solve (5)

---

1 **Initialization:** Initialize function value $\mathcal{F}_o = 0$, IRS phase shift matrices $\boldsymbol{\Theta}^j = \mathbf{I}$, control parameters $\boldsymbol{\alpha}$, $\boldsymbol{\beta}$, $\boldsymbol{W}$, and step size $\mu = 1$.

2 **while** $|\mathcal{F}_i - \mathcal{F}_{i+1}| \leq \epsilon$ **do**

3   Update $[\mathbf{V}_i^{\mathrm{RF}}, \mathbf{V}_i^{\mathrm{BB}}]$ by solving (9).

4   **repeat**

5   Compute Euclidean space gradient:
        $\nabla \mathcal{F} = \frac{\partial \mathcal{F}}{\partial \boldsymbol{\Theta}^*}(\boldsymbol{\Theta}^j)$.

6   Determine Riemannian space gradient direction:
        $\boldsymbol{J}(\boldsymbol{\Theta}^j) = \nabla \mathcal{F}(\boldsymbol{\Theta}^j)\boldsymbol{\Theta}^{j\,H} - \boldsymbol{\Theta}^j \nabla \mathcal{F}(\boldsymbol{\Theta}^j)^H$.

7   **if** $\|\boldsymbol{J}(\boldsymbol{\Theta}^j)\|_{\boldsymbol{\Theta}^j}^2$ *is sufficiently small* **then**

8   **break**.

9   **end**

10   Compute rotation matrices:
        $\boldsymbol{R}^j = \mathbf{I} + \mu\boldsymbol{J}^j + (\mu\boldsymbol{J}^j)^2/2 + (\mu\boldsymbol{J}^j)^3/6$,
        $\boldsymbol{U}^j = \boldsymbol{R}^j\boldsymbol{R}^j$.

11   Adjust μ to satisfy gradient reduction conditions using $\boldsymbol{R}^j$ and $\boldsymbol{U}^j$.

12   Update $\boldsymbol{\Theta}^{j+1} = \boldsymbol{J}(\boldsymbol{\Theta}^j)\boldsymbol{\Theta}^j$, increment j.

13   **until** *convergence*;

14   Store optimal value of $\boldsymbol{\Theta}$. Update $\mathcal{F}_i$ by solving (5a) and adjust auxiliary parameters as per section III-A.

15 **end**

TABLE I: Simulation Parameters

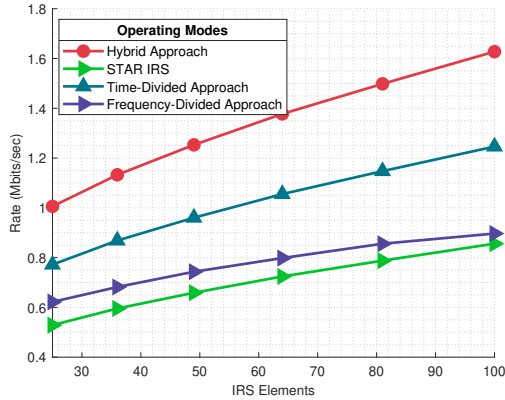| Parameter	Value	Parameter	Value
Area Length	$100m^2$ meters	N	4
f_c	$[0.1 - 1]$Thz	B	1MHz
N_o	-174 dBm/Hz	K	[25-100]
M	[49-225]	P_{max}	[15-30] dBm

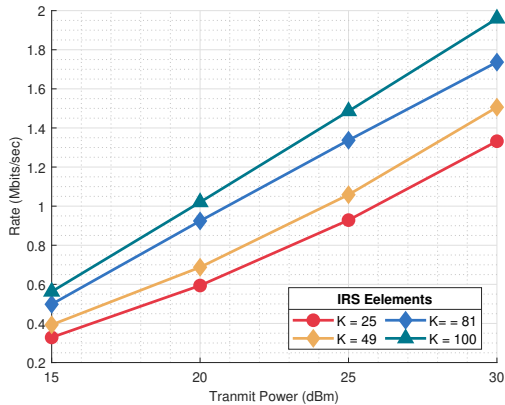Fig. 3: Operating Mode Vs IRS Elements
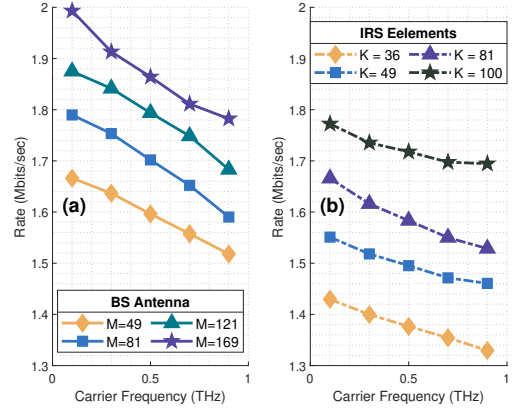

Fig. 4: Transmit Power Vs IRS Elements

Fig. 5: Carrier Frequency Vs BS Antennas

IV. PERFORMANCE EVALUATION

In this section, the performance of a fully connected BD-IRS to enhance THz communication systems is evaluated. We compare the hybrid transmissive/reflective design with two reference schemes: time-divided (TDMA) and frequency-divided (FDMA). In the former, IRS consecutively switches between transmissive and reflective mode to serve all the users. In the latter, two user groups are simultaneously served in two orthogonal frequency bandwidths. The results are also compared with those of the STAR IRS [20]. Furthermore, the analysis examines the impact of various simulation parameters, including the IRS performance across different frequency bands. Simulation parameters are listed in Table I.

The proposed scheme's effectiveness is determined by the algorithm's convergence. Through extensive simulation, average results are generated and plotted across different operating modes over iterations. Fig. 2 shows that, as the algorithm iterates, it converges to a stable point by setting $N_r = N_t$ and $M = K$. Notably, the proposed scheme outperforms others due to limitations in reflective and transmissive IRS configurations, respectively. Time-divided allows reflective and transmissive users to receive signals at different intervals, whereas frequency-division serves both user groups concurrently but at different bandwidths. In contrast, the hybrid approach allows for simultaneous service to both user sets, resulting in a higher average rate than alternatives.

The comparative analysis, illustrated in Fig. 3 under consistent settings, evaluates the efficacy of the hybrid approach against time-divided, frequency-divided strategies and STAR IRS across a range of IRS element counts. The findings underscore the distinct advantage of the fully connected hybrid approach, which surpasses the time-divided, frequency-divided, and STAR IRS methods by approximately 30.50%, 69.9% and 76.99%, respectively, demonstrating its notable superiority.

Fig. 4 illustrates the influence of transmit power and IRS elements on the system's performance. The results reveal that both factors contribute to enhancing system performance. Notably, increasing power levels exhibit a more pronounced effect on system performance compared to escalating the number of IRS elements. Specifically, power levels exhibit

an average percentage increase of 55.98%, while the increase attributable to IRS elements is approximately 11.94%.

Fig. 5 showcases the effects of carrier frequency and the number of BS antennas or IRS elements on system performance. The findings in 5a indicate that an increase in carrier frequency leads to higher absorption path loss, resulting in decreased performance. On average, an increase in carrier frequency leads to a system performance change of about -2.44%, whereas increasing the number of antennas results in an average performance improvement of approximately 5.44%. This underscores the beneficial role of additional antennas in enhancing system performance. Similarly, 5(b) presents consistent trends with varying numbers of IRS elements. Here, carrier frequency changes bring about a performance change of roughly -1.57%, and increasing the number of IRS elements leads to an average performance improvement of approximately 7.44% demonstrating its effectiveness as compared to BS antennas.

V. Conclusion

In conclusion, this research delineates the efficacy of implementing fully connected BD-IRS in a hybrid operational mode to enhance THz downlink communications and provide simultaneous service to both indoor and outdoor single-antenna users. For this, we formulate the joint optimization problem for hybrid beamforming at the THz BS along with the BD-IRS phase shifts to maximize the sum rate. Leveraging the conjugate gradient method, the research meticulously navigates the complexities of the optimization landscape, presenting a coherent strategy for addressing these challenges. Through rigorous numerical simulations, the results affirm the proposed method's substantial enhancement in system performance compared to traditional benchmarks, including time- and frequency-divided approaches and STAR-IRS, by demonstrating significant improvements in terms of rate by approximately 30.50% , 69.9% and 76.99%, respectively. This conclusive evidence underlines the proposed approach's efficacy and establishes a robust foundation for future advancements in THz communication networks. Future work may explore imperfect CSI and hardware limitations while enhancing energy efficiency in multi-user scenarios.

VI. Acknowledgement

References

[1] I. F. Akyildiz, C. Han, Z. Hu, S. Nie, and J. M. Jornet, "Terahertz band communication: An old problem revisited and research directions for the next decade," *IEEE Transactions on Communications*, vol. 70, no. 6, pp. 4250–4285, 2022.

[2] A. Mahmood, T. X. Vu, W. U. Khan, S. Chatzinotas, and B. Otter-sten, "Optimizing computational and communication resources for mec network empowered uav-ris communication," in *2022 IEEE Globecom Workshops (GC Wkshps)*. IEEE, 2022, pp. 974–979.

[3] Z. Zhu, J. Xu, G. Sun, W. Hao, Z. Chu, C. Pan, and I. Lee, "Robust beamforming design for IRS-aided secure SWIPT terahertz systems with non-linear EH model," *IEEE Wireless Communications Letters*, vol. 11, no. 4, pp. 746–750, 2022.

[4] C. Han, Y. Wu, Z. Chen, Y. Chen, and G. Wang, "THz ISAC: A physical-layer perspective of terahertz integrated sensing and communication," *IEEE communications magazine*, vol. 62, no. 2, pp. 102–108, 2024.

[5] A. Mahmood, T. X. Vu, W. U. Khan, S. Chatzinotas, and B. Ottersten, "Joint Computation and Communication Resource Optimization for Beyond Diagonal UAV-IRS Empowered MEC Networks," *arXiv preprint arXiv:2311.07199*, 2023.

[6] Q. Wu and R. Zhang, "Intelligent reflecting surface enhanced wireless network: Joint active and passive beamforming design," in *2018 IEEE Global Communications Conference (GLOBECOM)*, 2018, pp. 1–6.

[7] W. Hao, G. Sun, M. Zeng, Z. Chu, Z. Zhu, O. A. Dobre, and P. Xiao, "Robust design for intelligent reflecting surface-assisted MIMO-OFDMA terahertz IoT networks," *IEEE Internet of Things Journal*, vol. 8, no. 16, pp. 13 052–13 064, 2021.

[8] F. Zhao, W. Hao, X. You, Y. Wang, Z. Chu, and P. Xiao, "Joint Beamforming Optimization for IRS-aided THz Communication With Time Delays," *IEEE wireless communications letters*, 2023.

[9] J. Yuan, G. Chen, M. Wen, R. Tafazolli, and E. Panayirci, "Secure transmission for THz-empowered RIS-assisted non-terrestrial networks," *IEEE transactions on vehicular technology*, 2022.

[10] Huawei. Indoor digitalization with full connectivity. [Online]. Available: https://carrier.huawei.com/en/trends-and-insights/emsite/indoor-digitalization-with-full-connectivity

[11] Cisco. Cisco vision: 5g – thriving indoors whitepaper. [Online]. Available: https://www.cisco.com/c/dam/en/us/solutions/collateral/service-provider/ultra-services-platform/5g-ran-indoor.pdf

[12] Y. Xing, T. S. Rappaport, and A. Ghosh, "Millimeter wave and sub-THz indoor radio propagation channel measurements, models, and comparisons in an office environment," *IEEE Communications Letters*, vol. 25, no. 10, pp. 3151–3155, 2021.

[13] Y. Chen, C. Han, Z. Yu, and G. Wang, "Channel measurement, characterization and modeling for terahertz indoor communications above 200 ghz," *IEEE Transactions on Wireless Communications*, 2023.

[14] I. Yildirim, A. Uyrus, and E. Basar, "Modeling and analysis of reconfigurable intelligent surfaces for indoor and outdoor applications in future wireless networks," *IEEE transactions on communications*, vol. 69, no. 2, pp. 1290–1301, 2020.

[15] M. H. N. Shaikh, V. A. Bohara, A. Srivastava, and G. Ghatak, "An energy efficient dual IRS-aided outdoor-to-indoor communication system," *IEEE Systems Journal*, 2023.

[16] H. Li *et al.*, "Beyond diagonal reconfigurable intelligent surfaces: A multi-sector mode enabling highly directional full-space wireless coverage," *IEEE Journal on Selected Areas in Communications*, 2023.

[17] H. Li, S. Shen, and B. Clerckx, "Beyond diagonal reconfigurable intelligent surfaces: From transmitting and reflecting modes to single-, group-, and fully-connected architectures," *IEEE Transactions on Wireless Communications*, vol. 22, no. 4, pp. 2311–2324, 2022.

[18] M. Nerini *et al.*, "Discrete-value group and fully connected architectures for beyond diagonal reconfigurable intelligent surfaces," *IEEE Transactions on Vehicular Technology*, 2023.

[19] M. Soleymani *et al.*, "Optimization of rate-splitting multiple access in beyond diagonal RIS-assisted URLLC systems," *IEEE Transactions on Wireless Communications*, 2023.

[20] Z. Wang, X. Mu, J. Xu, and Y. Liu, "Simultaneously transmitting and reflecting surface (stars) for terahertz communications," *IEEE Journal of Selected Topics in Signal Processing*, 2023.

[21] T. L. Nguyen, T. N. Do, G. Kaddoum, D. B. da Costa, and Z. J. Haas, "Channel characterization for ris-aided terahertz communications: A stochastic approach," *IEEE Wireless Communications Letters*, vol. 11, no. 9, pp. 1890–1894, 2022.

[22] L. S. Rothman, I. E. Gordon, A. Barbe, D. C. Benner, P. F. Bernath, M. Birk, V. Boudon, L. R. Brown, A. Campargue, J.-P. Champion *et al.*, "The HITRAN 2008 molecular spectroscopic database," *Journal of Quantitative Spectroscopy and Radiative Transfer*, pp. 533–572, 2009.

[23] K. Shen and W. Yu, "Fractional programming for communication systems—part i: Power control and beamforming," *IEEE Transactions on Signal Processing*, vol. 66, no. 10, pp. 2616–2630, 2018.

[24] T. Abrudan, "Advanced optimization algorithms for sensor arrays and multi-antenna communications," Ph.D. dissertation, Department of Signal Processing and Acoustics, Aalto University, Finland, 21 Nov. 2008. [Online]. Available: http://lib.tkk.fi/Diss/2008/isbn9789512296071/